A mammalian PAR-3–PAR-6 complex implicated in Cdc42/Rac1 and aPKC signalling and cell polarity

Dan Lin*†, Amelia S. Edwards‡, James P. Fawcett*, Geraldine Mbamalu*, John D. Scott‡ and Tony Pawson*†§

*Program in Molecular Biology and Cancer, Samuel Lunenfeld Research Institute, Mount Sinai Hospital, 600 University Avenue, Toronto, Ontario M5G 1X5, Canada
†Department of Molecular and Medical Genetics, University of Toronto, Toronto, Ontario M5S 1A8, Canada
‡Howard Hughes Medical Institute, Vollum Institute, L474, Oregon Health Sciences University, 3181 Southwest Sam Jackson Park Road, Portland, Oregon 97201, USA
§e-mail: pawson@mshri.on.ca

Cellular asymmetry is critical for the development of multicellular organisms. Here we show that homologues of proteins necessary for asymmetric cell division in *Caenorhabditis elegans* associate with each other in mammalian cells and tissues. mPAR-3 and mPAR-6 exhibit similar expression patterns and subcellular distributions in the CNS and associate through their PDZ (PSD-95/Dlg/ZO-1) domains. mPAR-6 binds to Cdc42/Rac1 GTPases, and mPAR-3 and mPAR-6 bind independently to atypical protein kinase C (aPKC) isoforms. *In vitro*, mPAR-3 acts as a substrate and an inhibitor of aPKC. We conclude that mPAR-3 and mPAR-6 have a scaffolding function, coordinating the activities of several signalling proteins that are implicated in mammalian cell polarity.

Cellular polarity is critical to the development and function of many cell types. Polarized epithelial cells are organized into apical and basolateral domains, enabling these cells to carry out barrier and transport functions[1,2]. Polarized localization of proteins is also essential for asymmetric cell division during development. Asymmetric cell division involves the coordination of mitotic-spindle orientation with the polarity of the dividing cell to segregate localized proteins to one daughter cell but not the other[3–5]. The resulting division yields two daughter cells with different cell fates. Although the mechanism by which polarity is established is not fully understood, several proteins involved in this process have been identified. *C. elegans* PAR-3 and its homologue Bazooka in *Drosophila melanogaster* have an important function in asymmetric division and establishment of epithelial cell polarity[6].

The *par-3* gene is involved in asymmetric cell division early in *C. elegans* development[7]. In the polarized embryo, PAR-3 co-localizes with another PAR protein, PAR-6, and with the aPKC PKC-3, at the anterior pole[8–10]. However, other proteins, including PAR-1 and PAR-2, are restricted to the opposite pole[11,12]. Study of *par* mutants and analysis of *pkc-3* by RNA interference have shown that proper localization and function of these proteins are mutually interdependent[8–10,13,14]. In *par-3* mutants, for example, several asymmetrically distributed proteins are mislocalized, leading to disruption of mitotic-spindle orientation, of asymmetric cell division, and of cell-fate determination.

Bazooka has an analogous function in the development of the *Drosophila* nervous system. Neuroblast stem cells undergo asymmetric cell division to yield another neuroblast and a ganglion mother cell[15–17]. Bazooka forms a complex with Inscuteable (Insc) and Partner of Inscuteable (Pins) at the apical pole of the dividing neuroblast[18–23]. This complex is required for proper basal cortical localization of proteins such as the cell-fate determinants Numb and Prospero, and for correct orientation of the mitotic spindle in a manner reminiscent of PAR-3 function in the *C. elegans* embryo.

We previously isolated a murine PAR-3 homologue (PHIP) in a screen to identify binding partners for the carboxy-terminal tail of B-type ephrins[24]. For simplicity, we will refer to the murine homologue of PAR-3 as mPAR-3. A rat homologue of PAR-3/Bazooka, ASIP, has been identified as a component of both tight junctions and adherens junctions[25]. In addition, a cDNA clone encoding the murine homologue of PAR-6 (mPAR-6) has been identified in an expressed-sequence tag (EST) database[9].

Here we demonstrate that mPAR-3 can act as a scaffold to nucleate a multi-protein complex involving mPAR-6, the GTP-bound forms of Cdc42 and Rac1, and aPKC isoforms. Atypical PKCs have been shown to bind to PAR-3 and ASIP[10,25], and here we show that mPAR-3 can be phosphorylated by this kinase *in vitro* and that mPAR-6 can bind directly to aPKC. We provide evidence that one function of these interactions is to regulate aPKC activity. Lastly, the pattern of expression and subcellular distribution of mPAR-3 and mPAR-6 in the mammalian central nervous system (CNS) places the complex of interactions in a physiologically relevant context.

Results

Expression of mPAR-3 isoforms. We originally isolated an mPAR-3 complementary DNA in an expression screen to identify binding partners for the PDZ-domain-binding site of B-type ephrins[24]. A subsequent screen to obtain complete transcripts yielded cDNAs for two smaller splice variants, as well as the full-length transcript. All the splice forms share a common amino-terminal coding sequence but vary in the positions of their stop codons and in the sequences of their respective 3′ untranslated regions. Whereas the

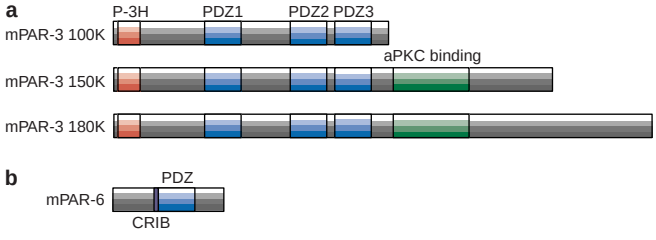

Figure 1 **Protein-domain organization of mPAR-3 and mPAR-6. a**, Schematic representations of the M_r 100K, 150K and 180K splice forms of mPAR-3. The PAR-3 homology region (P-3H), the 3 PDZ domains and the aPKC-binding region are shown. **b**, Schematic representation of mPAR-6. The CRIB motif and the single PDZ domain are shown.

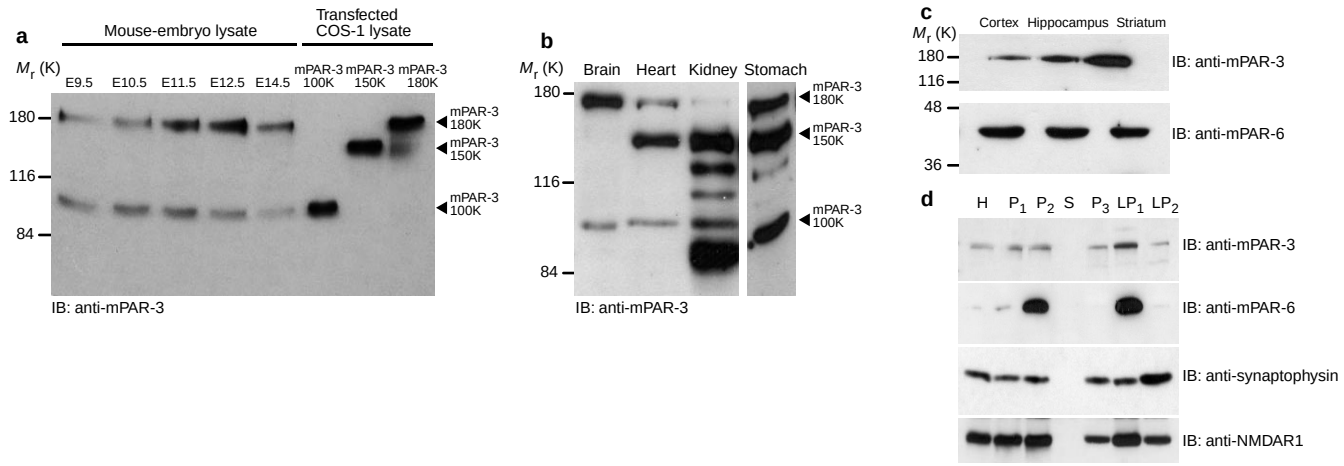

Figure 2 **Expression and subcellular distribution of mPAR-3 and mPAR-6. a**, Endogenous expression of mPAR-3 from E9.5 to E14.5 of mouse development and ectopic expression of mPAR-3 splice forms by transient transfection of COS-1 cells. Lanes were loaded with lysates from mouse embryo (50 μg) or COS-1 cells (5 μg), and immunoblotted (IB) with antisera raised against GST–mPAR-3 PDZ2+3 (anti-mPAR-3). The positions of relative-molecular-mass markers are shown on the left. **b**, Tissue-specific expression pattern of mPAR-3 isoforms in lysates of the indicated mouse adult tissues. Each lane was loaded with 50 μg total protein. **c**, mPAR-3 and mPAR-6 are co-expressed in the rodent brain. Equal amounts of lysate from rat cortex, hippocampus and striatum were analysed using antibodies against mPAR-3 and mPAR-6. Expression of mPAR-3 was highest in the striatum, with lower expression levels in the hippocampus and cortex. Expression of mPAR-6 was roughly uniform in each of the brain regions examined. **d**, Localization of mPAR-3 and mPAR-6 to a membrane fraction of lysed synaptosomes. A lysate of cortex from adult rats was fractionated by differential centrifugation and equivalent amounts of protein from each fraction were probed with the indicated antibodies. mPAR-3 was present in all fractions with the exception of a soluble fraction (S); levels were highest in an enriched membrane fraction obtained from lysed synaptosomes (LP1). The blot was stripped and reprobed with an anti-mPAR-6 antibody. Expression of mPAR-6 was observed in the homogenate (H) and the nuclear pellet (P1); levels were highest in the synaptosomal fraction (P2) and LP1. To assess the quality of fractionation, the distributions of two markers, the glutamate receptor NMDAR1 and the integral synaptic-vesicle membrane protein synaptophysin, were determined. Synaptophysin was present in all fractions except S and was especially enriched in a fraction containing microvesicles isolated from lysed synaptosomes (LP2). Highest levels of NMDAR1 were observed in the LP1 fraction. P_3 denotes a microsomal fraction.

full-length transcript encodes a protein of 1,337 amino acids, the two smaller transcripts contain open reading frames for proteins of 744 and 1,033 residues. All three proteins contain three PDZ domains, but the shortest isoform lacks the region that binds to aPKC isoforms (Fig. 1a). A search of the mouse EST database retrieved several sequences that match the three transcripts obtained from the cDNA screen, indicating that they may represent legitimate splice forms of mPAR-3. We cloned cDNAs for the splice forms into a mammalian expression vector and transfected them into COS-1 cells. Expression of the full-length transcript yielded a protein of relative molecular mass ~180,000 (M_r ~180K; mPAR-3 180K), whereas the two smaller cDNAs gave proteins of M_r 100K (mPAR-3 100K) and 150K (mPAR-3 150K; Fig. 2a).

To examine the expression of endogenous mPAR-3 isoforms during development and in the adult, we probed western blots of lysates from mouse embryo and adult tissue with an antibody raised against a region encompassing the second and third PDZ domains of mPAR-3, a segment common to all three isoforms. In the embryo, mPAR-3 180K and mPAR-3 100K were expressed at all time points examined, from day 9.5 of development (E9.5) to E14.5, whereas expression of mPAR-3 150K was not detectable (Fig. 2a). A survey of mPAR-3 expression in mouse adult tissues showed that the distribution of the splice forms was tissue-specific (Fig. 2b). For example, all three forms of mPAR-3 were present in the heart, whereas expression in the brain was limited primarily to the M_r 180K form and low levels of the M_r 100K form. Some tissues, such as the kidney, contained a large number of immunoreactive polypeptides, which may represent either further splice forms or proteolytic products.

mPAR-3 and mPAR-6 have similar expression patterns in the brain. In *C. elegans*, *par-3* and *par-6* exhibit a genetic interaction and the two proteins co-localize, indicating that mammalian mPAR-3 may physically interact with mPAR-6 (refs 9, 14). To

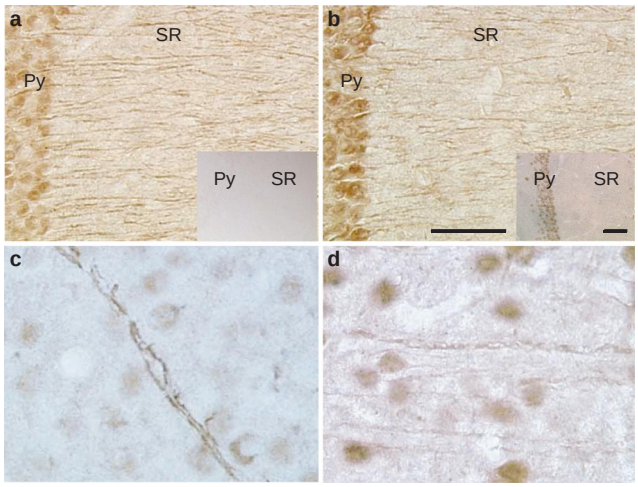

Figure 3 **Immunocytochemical localization of mPAR-3 and mPAR-6 in the adult mouse brain. a**, Positive mPAR-3 immunoreactivity in cellular and fibre profiles in the striatum radiatum (SR) of the CA1 region of the adult mouse hippocampus and in pyramidal neurons (Py). Staining was not visible in mouse brain treated with antibody pre-absorbed with excess GST–mPAR-3 PDZ2+3 (inset). **b**, Positive mPAR-6 immunoreactivity in fibre and cellular profiles in the SR of the CA1 region. Antigen competition using excess GST–mPAR-6 eliminated fibre staining, whereas nuclear staining was unaltered (inset). **c**, Positive mPAR-3 immunoreactivity localized to fibres in the cortex of adult mouse brain. Low-level staining of cellular profiles was also observed. **d**, Positive mPAR-6 immunoreactivity localized to fibre and cellular profiles in the adult mouse cortex. Scale bars represent 50 μm.

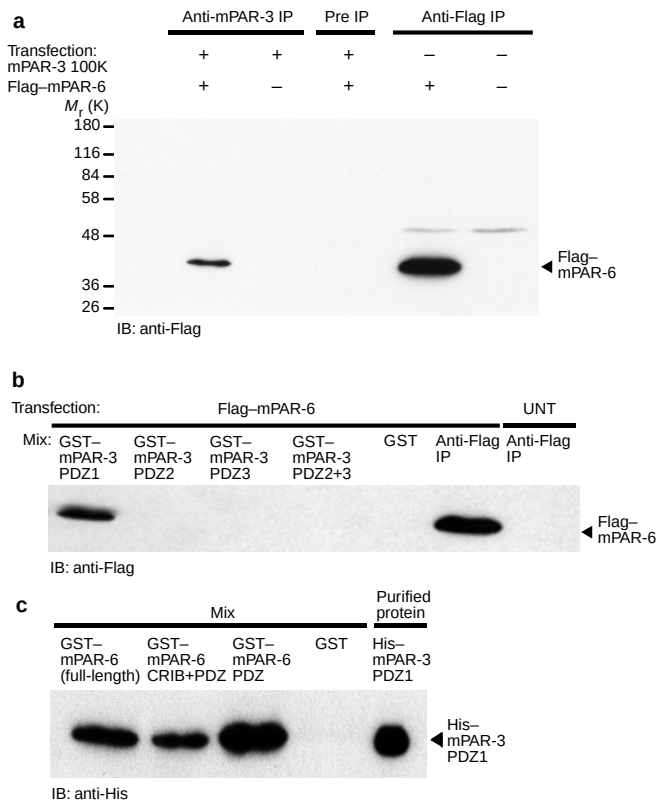

Figure 4 **mPAR-3 interacts with mPAR-6. a**, Co–immunoprecipitation of Flag–mPAR-6 with mPAR-3 100K. COS–1 cells were transfected with mPAR-3 100K and/or Flag–mPAR-6 as indicated. Proteins were immunoprecipitated (IP) from cell lysates with antibodies against mPAR-3, with pre-immune sera (Pre IP) or with antibodies against the Flag epitope. Immunoprecipitation of Flag–mPAR-6 by anti-Flag antibody was included as a positive control. Immunoprecipitates were immunoblotted (IB) with anti-Flag antibody. **b**, mPAR-6 binds specifically to mPAR-3 PDZ1. COS-1 cells were transiently transfected with Flag–mPAR-6 or were left untransfected (UNT). Cell lysates were incubated with the indicated GST-fusion proteins and analysed by immunoblotting with anti–Flag antibody. **c**, The interaction between mPAR-3 PDZ1 and mPAR-6 is direct and requires the PDZ domains. Purified mPAR-3 PDZ1 carrying a His epitope was incubated with purified, glutathione–sepharose-immobilized GST–mPAR-6 (full-length), GST–mPAR-6 CRIB+PDZ, GST–mPAR-6 PDZ or GST alone as indicated. Purified His–mPAR-3 PDZ1 (50 ng) was included as a positive control. Proteins were detected by immunoblotting with anti-His antibody.

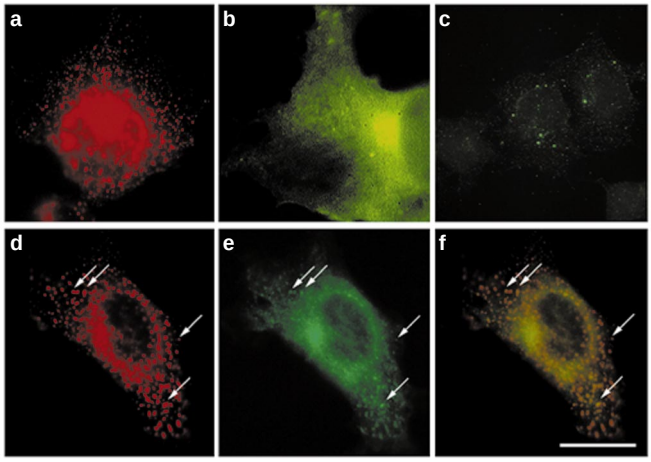

Figure 5 **Co-distribution of exogenous mPAR-3 100K and Flag–mPAR-6. a**, Anti-Flag staining (red) of a COS-1 cell transiently transfected with Flag–mPAR-6 alone. **b**, Anti-mPAR-3 staining (green) of a COS-1 cell exogenously expressing mPAR-3 100K alone. **c**, Antigen-competition control for mPAR-3 staining. Specific staining was not visible in samples treated with antibody pre-absorbed with excess GST–mPAR-3 PDZ2+3. **d**, Flag–mPAR-6 immunoflourescence staining in a COS-1 cell co-expressing exogenous Flag–mPAR-6 and mPAR-3 100K. **e**, Distribution of mPAR-3 100K in the same co-transfected COS-1 cell (arrows). **f**, Double staining of mPAR-3 100K (green) and Flag–mPAR-6 (red) in a cell ectopically co-expressing both proteins. Arrows in **d–f** show examples of co-distribution of mPAR-3 100K and Flag–mPAR-6. Scale bar represents 10 μM.

investigate this possibility, we characterized the expression of mPAR-3 and mPAR-6 in specific brain tissues by immunoblotting. The M_r 180K form of mPAR-3 was found to be expressed in adult rat cortex, hippocampus and at higher levels in the striatum (Fig. 2c). mPAR-6 was detected in the same tissues but at relatively uniform levels. These results confirm that mPAR-3 and mPAR-6 are both present in the same regions of the adult rat CNS.

As neurons are highly polarized, we investigated whether there is a specific subcellular distribution of mPAR-3 and mPAR-6 in CNS neurons. We used differential centrifugation to fractionate adult rat cortex and analysed each fraction by immunoblotting. Although mPAR-3 expression was evident in all fractions except the cytosol (S), it was enriched in a pellet fraction of lysed synaptosomes (LP1), which contained membrane-associated synaptosomal proteins and large amounts of the NMDA R1 glutamate receptor[26–28] (Fig. 2d). We stripped the same blot and re-probed it for mPAR-6. Although the expression pattern of mPAR-6 was similar to that of mPAR-3, mPAR-6 was particularly enriched in the P2 and LP1 fractions. These data indicate that mPAR-3 and mPAR-6 have similar subcellular distributions in the adult rat cortex.

To define the distribution of mPAR-3 and mPAR-6 in the rodent CNS more specifically, we carried out an immunocytochemical analysis of 35-μm coronal sections from adult mouse brain, focusing on the cortical and hippocampal regions. Positive fibre staining of mPAR-3 and mPAR-6 was observed in the cortex and in the striatum radiatum of the hippocampal CA1 region (Fig. 3). The distribution of fibre staining indicates that these two proteins may be localized within a similar neuronal population. Pre-incubation of the antibodies with excess amounts of their respective glutathione-*S*-transferase (GST)-fusion protein antigens abolished all fibre staining (Fig. 3, insets). These results indicate that mPAR-3 and mPAR-6 have similar cellular and subcellular distributions in the adult rodent CNS.

Association of mPAR-3 and mPAR-6 involves their PDZ domains. We addressed the question of whether mPAR-3 and mPAR-6 are able to interact physically, by co-transfecting COS-1 cells with mPAR-3 100K and full-length mPAR-6 tagged at its N terminus with a Flag epitope. Anti-mPAR-3 antibody specifically co-immunoprecipitated epitope-tagged mPAR-6 (Fig. 4a). We used immunofluorescence staining of COS-1 cells transfected with mPAR-3 100K and Flag–mPAR-6 to determine whether these two proteins co-localize. In cells transfected with Flag–mPAR-6 alone, anti-Flag staining showed a perinuclear and a punctate pattern showing partial co-distribution with alpha–mannosidase II, a marker for the Golgi apparatus, and with caveolin-1, a membrane raft protein (Fig. 5a and data not shown). In contrast, exogenous mPAR-3 100K alone was distributed throughout the cytoplasm in the majority of transfected cells (Fig. 5b). However, mPAR-3 100K exhibited a different localization in cells expressing both mPAR-3 100K and Flag–mPAR-6 (Fig. 5e). In line with the immunoprecipitation results, immunofluorescence staining of co-transfected COS-1 cells revealed a nearly complete co-distribution of mPAR-3 100K with Flag–mPAR-6 (Fig. 5f). We confirmed the specificity of mPAR-3 staining by antigen competition

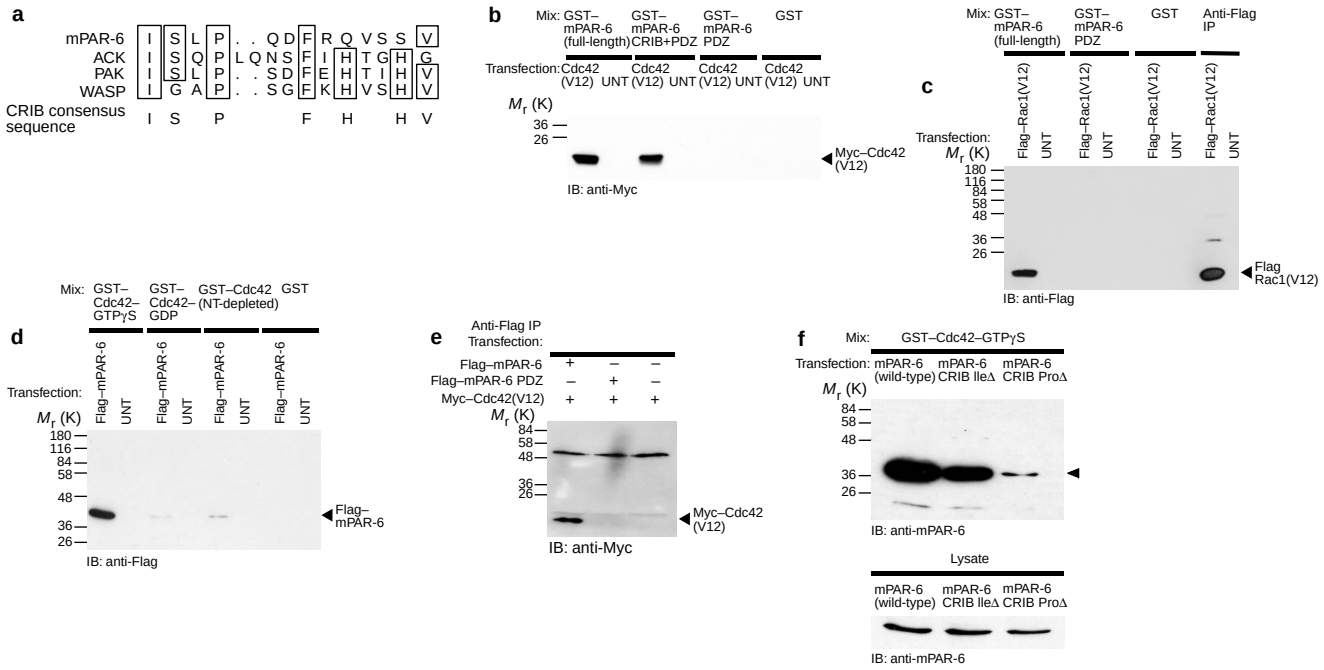

Figure 6 **mPAR-6 binds to Cdc42 and Rac1 through its CRIB motif. a**, Amino-acid sequences of the CRIB sites of mPAR–6, ACK, PAK and the Wiscott–Aldrich-syndrome protein (WASP). Conserved residues of the CRIB consensus sequence are boxed. **b**, GST–mPAR-6 (full-length) and the GST–mPAR-6 CRIB+PDZ fragment interact specifically with constitutively activated Myc–Cdc42(V12). Myc–Cdc42(V12) bound specifically to GST–mPAR-6 (full-length) and GST–mPAR-6 CRIB+PDZ immobilized on glutathione–sepharose. Neither a GST–mPAR-6 PDZ fragment, which lacks a complete CRIB sequence, nor GST alone exhibited detectable binding to Myc–Cdc42(Val12). UNT, untransfected. Proteins were detected by immunoblotting (IB) with anti-Myc antibody. **c**, GST–mPAR-6 (full-length) interacts specifically with constitutively activated Flag–Rac1(V12). Transfections and analysis were carried out as in **b**, except that GST–mPAR-6 CRIB+PDZ was not used, and expression of Rac1(V12) was verified by immunoprecipitation (IP) with anti-Flag antibody (far-right lane); anti-Flag antibody was also used for immunoblotting. **d**, mPAR-6 binds preferentially to Cdc42–GTPγS. GST-fusion proteins of full-length Cdc42, incubated either with non-hydrolysable GTPγS or with GDP or in nucleotide-free conditions (NT-depleted), were added to transfected COS-1 cell lysates. Proteins were detected by immunoblotting with anti-Flag antibody. **e**, Cdc42(V12) co-immunoprecipitates with full-length mPAR-6 but not with an mPAR-6 PDZ domain fragment. COS-1 cells were co-transfected with Myc–Cdc42(V12) and Flag-tagged mPAR-6 (full-length) or mPAR-6 PDZ. Cell lysates were immunoprecipitated with anti-Flag antibody and the blot was probed with anti-Myc antibody. **f**, Deletion of Pro136 in the mPAR-6 CRIB sequence (mPAR-6 CRIB ProΔ) strongly reduces binding to GST–Cdc42–GTPγS. Loss of Ile133 (mPAR-6 CRIB IleΔ) does not significantly affect binding in comparison to wild-type mPAR-6. The indicated transfections were carried out and proteins were detected by immunoblotting with anti-mPAR-6 antibody (upper panel). Bands corresponding to mPAR-6 are marked with an arrowhead. Lower panel, cell lysates were probed with anti-mPAR-6 antibody to compare expression levels.

(Fig. 5c). These data indicate that mPAR-3 100K and mPAR-6 associate with one another in cells.

Both mPAR-3 and mPAR-6 contain PDZ domains, raising the possibility that the two proteins may interact by PDZ-domain heterodimerization. We incubated GST-fusion proteins, consisting of either the first, second or third PDZ domains of mPAR-3, with lysates of COS-1 cells transfected with Flag–mPAR-6. We subjected the resulting complexes to western blotting using antibodies against the Flag epitope of mPAR-6. Full-length mPAR-6 bound specifically to the first PDZ domain of mPAR-3, but not to fusions of the other two PDZ domains or to GST alone (Fig. 4b). To determine whether this interaction is direct, we incubated purified histidine (His)-tagged mPAR-3 PDZ1 protein with GST-fusion proteins of mPAR-6 bound to glutathione beads. mPAR-3 PDZ1 associated with GST–mPAR-6 (full-length) but not with GST alone, indicating that the two proteins can associate directly. Two internal fragments of mPAR-6, containing the single central PDZ domain and lacking the C-terminal sequence (GST–mPAR-6 CRIB+PDZ and GST–mPAR-6 PDZ) also bound to mPAR-3 PDZ1. This demonstrates that the PDZ domains are sufficient for mPAR-3–mPAR-6 interaction.

mPAR-6 contains a functional CRIB motif. Comparison of the sequences of PAR-6 homologues has revealed a segment of conserved residues reminiscent of a CRIB site (Figs 1b, 6a; I. Macara, personal communication). CRIB motifs are short sequences that bind to activated forms of Cdc42 and Rac GTPases[29]. Interestingly, the putative CRIB sequence of mPAR-6 lacks two conserved histidine residues that are present in all other CRIB sequences. To investigate whether mPAR-6 can bind to activated Cdc42, we incubated GST-tagged, full-length mPAR-6 with lysates of COS-1 cells transfected with a Myc-tagged Val12 mutant of Cdc42 (Cdc42(V12)), which is constitutively active in the GTP-bound state. Immunoblotting showed that mPAR-6 specifically bound to Cdc42(V12) (Fig. 6b). A GST–mPAR-6 CRIB+PDZ fragment, which contains the full sequence of the putative CRIB site, also bound to Cdc42(V12). In contrast, neither GST alone nor the GST–mPAR-6 PDZ fragment, which contains only the C-terminal half of the CRIB sequence, exhibited detectable binding. Similar results were obtained with an activated Rac1 Val12 mutant tagged with a Flag epitope (Fig. 6c and data not shown). In a complementary experiment, a GST fusion of wild-type Cdc42 was treated with non-hydrolysable GTPγS or with GDP, or was nucleotide-depleted, and then assayed for binding to full-length mPAR-6. In comparison with the GDP-bound or nucleotide-depleted forms, the GTPγS-bound form of Cdc42 preferentially bound *in vitro* to full-length mPAR-6 (Fig. 6d). A GST fusion of Rac1–GTPγS behaved in a similar manner (data not shown).

We also assayed the interaction between activated Cdc42 and

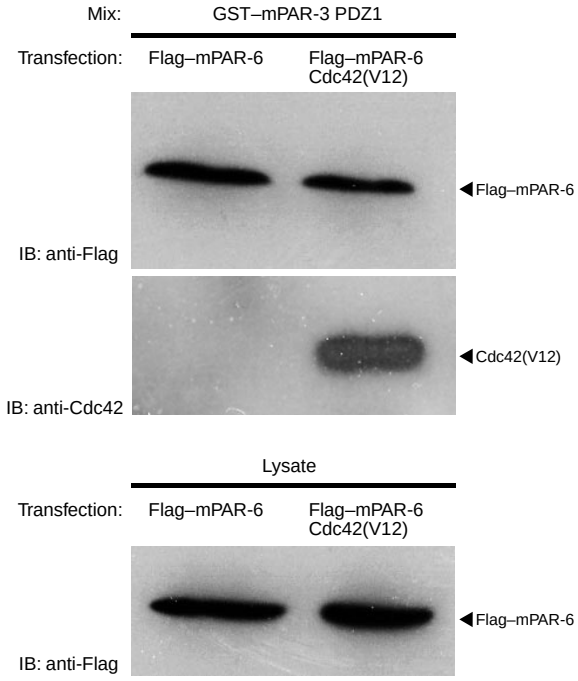

Figure 7 **mPAR-3 PDZ1, mPAR-6 and Cdc42(V12) can form a ternary complex.** Lysates of COS-1 cells co–transfected with Flag–mPAR-6 and Cdc42(V12) or transfected with Flag–mPAR-6 alone were incubated with GST–mPAR-3 PDZ1 and the resulting complex was analysed by immunoblotting (IB) with anti–Flag antibody (upper panel). The blot was stripped and reprobed for Cdc42 to determine whether Cdc42(V12) is present in the complex (middle panel). Cell lysates were probed with anti-Flag antibody to compare levels of Flag–mPAR-6 expression (lower panel).

mPAR-6 by co-immunoprecipitation studies using COS-1 cells exogenously expressing both Myc-tagged Cdc42(V12) and Flag-tagged mPAR-6. Cdc42(V12) specifically co-immunoprecipitated with full-length mPAR-6, but not with the mPAR-6 PDZ fragment (Fig. 6e), which lacks the intact CRIB-like motif. This indicates that a functional CRIB-like sequence may be required for binding of Cdc42 and Rac1 to mPAR-6. To examine this possibilty, we transfected COS-1 cells with wild-type mPAR-6 or with mutants lacking conserved CRIB residues, and assayed for binding to GST-Cdc42–GTPγS in cell lysates. Whereas deletion of Ile133 had little effect on binding of GST–Cdc42–GTPγS to mPAR-6, removal of the conserved proline residue at position 136 strongly inhibited this interaction (Fig. 6f). Expression levels of both mutant mPAR-6 proteins were comparable to that of the wild type. These results indicate that mPAR-6 interacts specifically with GTP–bound forms of both Cdc42 and Rac1 in a manner that is at least partially dependent on residues in the CRIB sequence.

As mPAR-6 associates with mPAR-3, we tested whether these proteins could form a ternary complex with activated Cdc42. We incubted lysates of COS-1 cells co-transfected with mPAR-6 and Cdc42(V12) with a GST–mPAR-3 PDZ1 fusion protein. Cdc42(V12) was precipitated with mPAR-6 by mPAR-3 PDZ1, indicating that mPAR-3, mPAR-6 and activated Cdc42 can form a tripartite complex (Fig. 7).

mPAR-3 is an inhibitor of aPKC *in vitro*. The two aPKC isoforms, PKCζ and PKCι/λ, have previously been identified as direct binding partners for ASIP, the rat homologue of mPAR-3 (ref. 25). In light of the observed co-localization of mPAR-3 and mPAR-6 in the CNS, we investigated whether the aPKC isoforms associate with mPAR-3 and mPAR-6 in the brain. In co-immunoprecipitation and GST-mixing experiments, PKCι/λ was specifically precipitated from lysates of adult rat brain by anti-mPAR-3 antibodies and by a GST-fusion protein consisting of the aPKC-interacting region of mPAR-3 (GST–mPAR-3(747–956); Fig. 8a). GST-fused full-length mPAR-6 also precipitated PKCι/λ from brain lysates (data not shown). From these experiments, however, we were not able to determine whether the interaction between mPAR-6 and aPKC isoforms was direct or was exclusively mediated by endogenous mPAR-3. To distinguish between these two possibilities, we used purified proteins. GST-fused full-length mPAR-6 bound to purified PKCζ *in vitro*, indicating that mPAR-6 binds directly to aPKC isoforms, independently of mPAR-3 (Fig. 8b). Using GST fusions of defined fragments of mPAR-6, we determined that the N–terminal portion of mPAR-6 (residues 1–100) is both necessary and sufficient for interaction with aPKCs (data not shown). Thus, aPKCs could potentially form a bridge between mPAR-3 and mPAR-6. As noted above, this is not the only mechanism by which mPAR-3 and mPAR-6 can interact, as they can associate directly through their PDZ domains. Furthermore, the M_r 100K mPAR-3 isoform lacks the aPKC-binding site but nevertheless interacts with mPAR-6.

Given that mPAR-3 and mPAR-6 can associate with aPKC isoforms, we investigated the possibility that either protein could act as a substrate for this enzyme. We carried out *in vitro* kinase assays by incubating purified PKCζ with GST–mPAR-3(747–956) and GST–mPAR-6, and identified the resulting phosphorylated proteins by autoradiography. GST–mPAR-3(747–956) was strongly phosphorylated by PKCζ (Fig. 8c). In contrast, little or no phosphorylation of mPAR-6 was detected. On the basis of these results, mPAR-3 seems to be a likely substrate for aPKC isoforms.

The mPAR-3(747–956) fragment contains two highly conserved serine residues, at positions 827 and 829, that represent potential binding and phosphorylation sites for aPKC. To evaluate the significance of these residues, we mutated them to either alanine or to glutamic acid. The double-alanine and double-glutamic-acid mutations effectively abrogated binding of mPAR-3(747–956) to PKCι/λ, as determined in GST-mixing experiments (Fig. 8a). Phosphorylation of mPAR-3(747–956) fragment was also substantially reduced in both double mutants, indicating that residues 827 and 829 may constitute important phosphorylation sites for aPKC (Fig. 8c).

To determine whether mPAR-3 and mPAR-6 have an effect on the activity of aPKCs, we carried out *in vitro* kinase assays using protamine as an exogenous substrate. We separately added GST–mPAR-3(747–956), GST–mPAR-6 and GST alone to purified PKCζ in the presence or absence of protamine. As a control, we excluded the protamine substrate from the reaction, to measure the level of phosphorylation of each GST fusion protein by PKCζ. In line with our earlier findings, phosphorylation of GST–mPAR-3(747–956) was observed, whereas no significant PKCζ activity towards GST or GST–mPAR-6 was detected (Fig. 8d, open columns). To measure the effect of each fusion protein on an exogenous substrate, we added protamine to each reaction and measured PKCζ activity (Fig. 8d, filled columns). In the presence of protamine, addition of GST–mPAR-3(747–956) reduced PKCζ activity by ~40% relative to levels observed with GST alone, indicating that interaction with mPAR-3 may hold aPKC in an inactive conformation. Interestingly, mPAR-6 had little effect on PKCζ activity, and, if anything, induced a modest increase in kinase activity towards protamine. These data indicate that the activation state of aPKC may be differentially regulated through binding to mPAR-3 and mPAR-6.

Discussion

Many of the invertebrate proteins involved in control of polarity and asymmetric cell division are composed of modular domains that are implicated in protein–protein interactions, and may therefore form multi-protein complexes that determine cellular asymmetry. Using the mammalian homologues of two invertebrate cell-fate

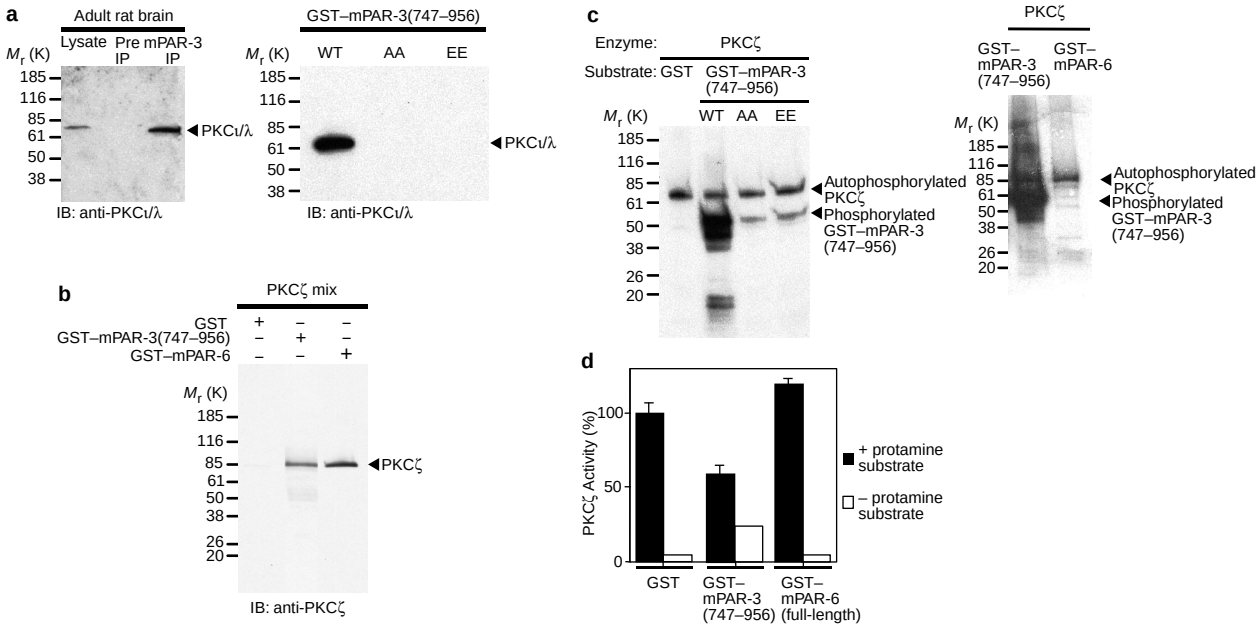

Figure 8 **mPAR-3 and mPAR-6 both bind directly to aPKC and affect its activity. a**, Left panel, endogenous PKCι/λ from rat brain co-immunoprecipitates with mPAR-3. Lysates and immunopecipitates (IP), with pre-immune sera or anti-mPAR-3 antibody, from adult rat brain were immunoblotted (IB) with anti-PKCι/λ antibody. Right panel, GST–mPAR-3(747–956) (wild-type, WT) binds to PKCι/λ from rat brain. GST–mPAR-3(747–956) containing double serine-to-alanine (AA) or serine-to-glutamic-acid (EE) mutations at residues 827 and 829 do not bind to endogenous PKCι/λ. Proteins were detected by immunoblotting with anti-PKCι/λ antibody. **b**, Purified PKCζ interacts directly with either GST–mPAR-6 (full-length) or GST–mPAR-3(747–956) in an *in vitro* mixing experiment. Proteins were detected by immunoblotting with anti-PKCζ antibody. **c**, aPKC phosphorylates GST–mPAR-3(747–756) *in vitro*. Kinase assays were carried out using purifed PKCζ together with GST alone, GST–mPAR-6 or GST–mPAR-3(747–956) (wild-type or the AA or EE mutants). Bands corresponding to autophosphorylated PKCζ and phosphorylated GST–mPAR-3(747–956) are marked. Phosphorylation of the double mutants is significantly reduced compared with that of the wild type. The lower bands represent phosphorylation of degradation products. **d**, Activity of aPKC is inhibited by mPAR-3, but not mPAR-6, *in vitro*. PKCζ was incubated in the presence (filled columns) or absence (open columns) of the exogenous substrate protamine. GST alone, GST–mPAR-6 (full-length) or GST–mPAR-3(747–956) (1.5μM) were included in the reaction and PKCζ activity was assayed by incorporation of ^{32}P onto protamine or the GST-fusion proteins. PKCζ activity is expressed relative to the level of ^{32}P incorporation in the presence of protamine and GST alone. The increase in PKCζ activity in the absence of protamine observed for GST–mPAR-3(747–956) is due to phosphorylation of mPAR-3 by PKCζ. Data are means ± s.e.m. from three separate experiments.

determinants, we have identified such a complex, involving the PDZ-domain proteins mPAR-3 and mPAR-6, the Cdc42/Rac1 GTPases, and aPKC.

The four components of the assembly apparently undergo complex interactions that may regulate the activation of pathways controlling polarity and spindle orientation. Furthermore, as several of the interaction modules in the complex still lack known binding partners, it is likely that further components of this regulatory apparatus remain to be identified. For example, the physiological binding partners for the PDZ2 and PDZ3 domains await identification, although the B-type ephrins are potential *in vivo* ligands for PDZ3 (ref. 24).

An important interaction in the complex seems to be the association of the PDZ domains of mPAR-3 and mPAR-6. This interaction is apparently direct, potentially involving a head-to-tail orientation similar to that described for the nNOS and syntrophin PDZ domains[30]. The observed co-localization of mPAR-3 and mPAR-6 in transfected cells and their similar staining patterns and subcellular distributions in the CNS indicate that their association may be physiologically important. The presence of both proteins in the synaptosomal fraction is consistent with a possible function in neuronal organization in the CNS. Neurons are highly polarized cells, the asymmetry of which shows similarities to epithelial cell polarity and prompts comparison of the axonal and somatodendritic surfaces of neurons to the apical and basolateral domains of epithelial cells[31–33]. It will be of interest to investigate whether mPAR-3 and mPAR-6 are involved in determining the plane of division in mitotic ventricular neural progenitors, which in turn determines subsequent cell fate[34]. Similarly, expression of mPAR-3 in the developing mouse embryo raises the possibility that this protein has an important function in early embryogenesis in mammals as well as in invertebrates.

The specific binding of mPAR-6 to activated Cdc42/Rac1 through its CRIB-like motif identifies a new component that potentially links the mPAR-3–mPAR-6 complex to signalling pathways that are involved in regulation of the actin cytoskeleton. Members of the Rho family of GTPases function as molecular switches in diverse cellular events, notably cytoskeletal organization[35,36]. During asymmetric cell division in early *C. elegans* embryos, cytoskeletal rearrangements are required for polarity, and treating embryos with cytochalasin D results in defects similar to those observed in *par* mutants[37,38]. A growing body of evidence has implicated both Rac1 and Cdc42 in establishment of epithelial cell polarity. Expression of constitutively active and dominant negative forms of Rac1 in MDCK cells disrupts the barrier function of epithelial cells by causing defects in tight junctions[39]. Interestingly, the endogenous mPAR-3 150K and 180K isoforms localize to junctional complexes in epithelial cells (data not shown), as does rat ASIP[25]. Functional deletion of Cdc42 in MDCK cells leads to mislocalization of membrane proteins that are normally found at the basolateral surface, indicating that Cdc42 has a function in maintenance of epithelial polarity in these cells[40].

As Cdc42 must be in the GTP-bound form to efficiently recognize mPAR-6, and it can form a tripartite complex with mPAR-3 and mPAR-6, it seems likely that activation of Cdc42 serves to regulate mPAR-3/mPAR-6 signalling. This might be achieved by simple

relocalization of the complex to membrane sites where Cdc42 is concentrated. In addition, Ccd42 might cause a conformational change in mPAR-6 that regulates its association with other partners and may influence aPKC activity.

The fact that both mPAR-3 and mPAR-6 interact with aPKC indicates that one output of the complex may be in the form of aPKC phosphorylation of substrates. The region of mPAR-3 that binds to aPKC contains serine residues that seem to be substrates for aPKC kinase activity and are required for association of the kinase with mPAR-3. As mPAR-3 seems to repress aPKC activity *in vitro*, it is possible that mPAR-3 acts as a scaffold to maintain aPKC in a latent state by binding to its catalytic domain. mPAR-6 binds to aPKC independently of mPAR-3 but seems to support full aPKC activity. Thus, it is conceivable that aPKC, once released from its mPAR-3 anchor, may remain tethered to the complex through its association with mPAR-6, but in an enzymatically active form. It will be interesting to determine the exent to which signals that potentially influence aPKC activity, such as phosphatidylinositol-3-kinase function[41,42], influence mPAR-3/mPAR-6 signalling.

Finally, it is worth noting that mPAR-3–mPAR-6 complexes may be highly dynamic in nature. This possibility is indicated by the identification of several isoforms of mPAR-3, which are differentially expressed in different tissues and have distinct binding activities, notably the lack of an aPKC-binding region in the M_r 100K isoform. □

Methods

Constructs, mutagenesis, fusion proteins and antibodies.

Library screening to isolate mPAR-3 cDNAs was carried out as described[24]. Full-length mPAR-6 cDNA was obtained from mouse EST clone 440139 (Genome Systems, St Louis, Missouri). cDNAs for the three splice forms of mPAR-3 and for mPAR-6 were subcloned into the pcDNA3 mammalian expression vector (Invitrogen) using standard cloning procedures. Full-length mPAR-6 and mPAR-6 PDZ (residues 138–298) were subcloned in frame into pFLAG CMV2 (Kodak). For GST-fusion constructs, cDNA sequences of mPAR-3 (PDZ1, residues 246–363; PDZ2, residues 457–598; PDZ3, residues 582–714; PDZ2+3, residues 457–744; aPKC-interacting region, residues 747–956) and mPAR-6 (full-length, residues 1–346; CRIB+PDZ, residues 117–298; PDZ, residues 138–298) were cloned in frame into pGEX vectors (Amersham). For His-tagged constructs, the cDNA sequence of mPAR-3 (PDZ1, residues 246–363) was cloned into pPRO EX HTa (Life Technologies). Mutations in mPAR-3 and mPAR-6 cDNAs were generated using the QuikChange site-directed mutagenesis kit (Stratagene). All fusion constructs and mutations were confirmed by sequencing. GST and His-tag fusion proteins were expressed in *Escherichia coli* strain BL21 and purified using standard procedures. GST fusions of Cdc42 were prepared and loaded with either GTPγS, GDP or were nucleotide depleted as described[43,44]. Briefly, GST–Cdc42 was prepared and incubated in buffer A (20 mM Tris–HCl pH 7.5, 1 mM dithiothreitol, 10 mM EDTA, 50 mM NaCl, 5% glycerol, 0.1% Triton X-100, 10 μg ml^{-1} leupeptin and 10 μg ml^{-1} aprotonin) at room temperature for 1 h to establish a guanine-nucleotide-free state. The sample was divided into three aliquots and each aliquot was incubated in either buffer A, buffer B (buffer A with 10 mM $MgCl_2$ and 120 μM GDP substituted for 10 mM EDTA) or buffer C (buffer B with 120 μM GTPγS substituted for 120 μM GDP) for 30 min at room temperature to establish the nucleotide-free, GDP-bound and GTPγS-bound states. Rabbit polyclonal antibodies were raised separately against GST fusions of mPAR-3 PDZ2+3 and mPAR-6 PDZ. Antibodies against mPAR-3 and mPAR-6 were affinity-purified by applying raw sera through a GST–sepharose column to remove anti-GST antibodies, and then running them over either a GST–mPAR-3 PDZ2+3 or a GST–mPAR-6 PDZ sepharose column. Mouse monoclonal anti-Flag M2, rabbit polyclonal anti-NMDA NR1 and mouse monoclonal anti-synaptophysin antibodies were from Eastman Kodak, Upstate Biotechnology and Sigma, respectively. Mouse monoclonal anti-Myc (9E10), and goat polyclonal anti-PKCζ antibodies were from Santa Cruz. Mouse monoclonal anti-tetra-His antibodies were from Qiagen. Mouse monoclonal anti-PKCι/λ antibodies were from Transduction Laboratories.

Subcellular fractionation.

Subcellular fractionation was carried out by differential centrifugation as described[45,46]. Briefly, the cortex was removed from adult rats and homogenized (H) in 10 mM HEPES–OH buffer, pH 7.3, containing 320 mM sucrose, 1 mM phenylmethylsulfonyl fluoride (PMSF), 10 μg ml^{-1} aprotinin, 0.2 μg ml^{-1} leupeptin and 1.5 mM sodium vanadate. Crude synaptosomes (P2) were separated from cytosol (S) and microsomes (P3) by differential centrifugation of a postnuclear supernatant. Synaptosomes were disrupted by hypotonic shock and quickly returned to osmotic balance by addition of 1 M HEPES, pH 7.4. Enriched synaptosomal membranes (LP1) were separated from the supernatant of lysed synaptosomes (LS1) by centrifugation at 25,000*g*. The LS1 supernatant was centrifuged at 260,000*g* to isolate a microsomal fraction (LP2). Small aliquots from each fraction were kept for protein determination using the bicinchoninic acid kit (BCA, Pierce).

Immunoprecipitation and western blotting.

For biochemical analysis of mPAR-3 and mPAR-6 in brain tissue, the cortex, hippocampus and striatum from adult rat brains were dissected separately, homogenized, and lysed at 4 °C in Tris-buffered saline (TBS) lysis buffer containing 137 mM NaCl, 20 mM Tris pH 8.0, 1% (*v*/*v*) NP-40, 10% (*v*/*v*) glycerol, 1 mM PMSF, 10 μg ml^{-1} aprotinin, 0.2 μg ml^{-1} leupeptin and 1.5 mM sodium vanadate. Mouse adult organs were dissected and lysed at 4 °C in phospholipase C lysis (PLC) buffer containing 10 μg ml^{-1} aprotonin, 10 μg ml^{-1} leupeptin, 1 mM sodium vanadate and 1 mM PMSF[47]. After lysis, all homogenates were spun at 15,000*g* for 30 min at 4 °C. The supernatant was collected and respun at 13,000 r.p.m. for a further 15 min at 4 °C. All lysates were boiled in sample buffer containing 2-mercaptoethanol, and 50 μg of protein was separated by SDS–PAGE.

COS-1 cells were cultured in DMEM supplemented with 10% FBS. Transient transfections were carried out using Lipofectin reagent and Opti-MEM medium (Life Technologies) according to the manufacturer's instructions. Transfected cells were rinsed once in phosphate-buffered saline (PBS) and lysed in PLC lysis buffer with 10 μg ml^{-1} aprotonin, 10 μg ml^{-1} leupeptin, 1 mM sodium vanadate and 1 mM PMSF. Immunoprecipitations were carried out for 2 h at 4 °C, using antibody at a concentration of 1 μg ml^{-1} with either protein A or goat anti-mouse sepharose. GST-mixing experiments were carried out by 2-h incubation of lysates at 4 °C with 5–10 μg of fusion protein immobilized on glutathione–sepharose. To measure direct binding of mPAR-3 PDZ1 to mPAR-6, 5 μg of purified His–mPAR-3 PDZ1 was incubated with 5 μg of purified GST–mPAR-6 fusion proteins bound to glutathione–sepharose. To assay direct binding of GST–mPAR-3(747–956) and GST–mPAR-6 to PKCζ, 200 ng of purified PKCζ (Calbiochem) was incubated with the fusion proteins bound to glutathione–sepharose. Beads for both immunoprecipitations and GST-mixing experiments were washed three times in HNTG buffer[47]. For GST–Cdc42-mixing experiments, beads were washed in buffer A, B or C to maintain the nucelotide-free, GDP-bound and GTPγS-bound states, respectively. Proteins were separated by SDS–PAGE, transferred to Immobilon–P membrane (Millipore), and immunoblotted with the appropriate antibody. Blots were developed by enhanced chemiluminescence (Pierce).

Immunocytochemistry.

Adult mice were killed with sodium pentobarbital (65 mg kg^{-1}) and transcardially perfused with 0.1 M phosphate buffer, pH 7.4, and then with 4% paraformaldehyde in phosphate buffer. Brains were then removed and post-fixed overnight in 4% paraformaldehyde in phosphate buffer at 4 °C. Brains were cryoprotected in graded sucrose solutions and sectioned on a cryostat before immunocytochemical analysis. Sections of 35-μm thickness were rinsed well in phosphate buffer and submerged in blocking solution containing 10% normal goat serum (NGS) and 0.2% Triton X-100 in phosphate buffer for 1 h at room temperature. Sections were transferred to primary antibody (anti-mPAR-3, 0.5 μg ml^{-1} or anti-mPAR-6, 1.5 μg ml^{-1}) in blocking solution and left overnight at 4 °C. Sections were washed 3 times (15 min each) in phosphate buffer and transferred to biotin-conjugated goat anti-rabbit antibody (1/200) in blocking solution for 1 h at room temperature. Sections were washed a further three times then incubated in ABC solution (Vector Laboratories, Burlingame, California) according to the manufacturer's recommendations. After incubation for 1 h, sections were washed as above, and immunopositive staining was visualized using diaminobenzadine reagent.

Immunofluorescence staining was carried out on transfected COS-1 cells seeded onto glass cover slips. Cells were rinsed briefly in PBS, fixed with 4% paraformaldehyde in PBS for 15 min, permeabilized with 0.1% Triton X-100 in PBS for 5 min and placed in blocking solution (5% BSA, 5% NGS and 0.01% Tween20 in PBS) for 1 h at room temperature. A double-label immunofluorescence-staining procedure was used to detect exogenous mPAR-3 100K and Flag–mPAR-6. Samples were incubated with primary antibodies (1.0 μg ml^{-1} anti-mPAR-3 and 1.0 μg ml^{-1} anti-Flag) in blocking solution for 1 h at room temperature. FITC-conjugated anti-rabbit and Texas-Red-conjugated anti-mouse antibodies (Molecular Probes) were used to detect the primary antibodies. All samples were mounted in a 50% glycerol/PBS solution supplemented with p-phenylenediamine to retard photobleaching. Microscopy was carried out using a Leica DMRX microscope equipped with fluorescence optics. Antigen-competition experiments were carried out by incubating 20 μg of affinity-purified antibody with 2 mg of their respective GST-fusion-protein antigens immobilized on sepharose beads overnight at 4 °C. Beads were pelleted by centrifugation and the supernatant was used for immunostaining as described above.

In vitro kinase assays.

The activity of PKCζ (Calbiochem) was assayed by measuring the rate of phosphorylation of protamine sulphate in the presence of 1.5 μM of various GST-purified proteins. The reaction mixture (80 μl) contained 50 μM protamine sulphate, 1 mM dithiothreitol, 0.1 mM [γ-^{32}P]ATP (0.1 μCi nM^{-1}) and 5 mM $MgCl_2$ in 20 mM HEPES, pH 7.5. Samples were incubated at 30 °C for 6 min and quenched by addition of 25 μl of a solution containing 0.1 mM ATP and 0.1 mM EDTA, pH 8–9. Aliquots (80 μl) were spotted on P81 ion-exchange chromatography paper, washed 4 times with 0.4% (*v*/*v*) phosphoric acid and rinsed with 95% ethanol; incorporation of ^{32}P was detected by scintillation counting. For gel assays, the same assay was carried out and halted with SDS–PAGE running buffer. Incorporation of ^{32}P was detected by autoradiography.

RECEIVED 13 MARCH 2000; REVISED 8 MAY 2000; ACCEPTED 15 JUNE 2000;
PUBLISHED 17 JULY 2000.

1. Yeaman, C., Grindstaff, K. K. & Nelson, W. J. New perspectives on mechanisms involved in generating epithelial cell polarity. *Physiol. Rev.* **79,** 73–98 (1999).
2. Cereijido, M., Valdes, J., Shoshani, L. & Contreras, R. G. Role of tight junctions in establishing and maintaining cell polarity. *Annu. Rev. Physiol.* **60,** 161–177 (1998).
3. Guo, S. & Kemphues, K. J. Molecular genetics of asymmetric cleavage in the early *Caenorhabditis elegans* embryo. *Curr. Opin. Genet. Dev.* **6,** 408–415 (1996).
4. Lin, H. & Schagat, T. Neuroblasts: a model for the asymmetric division of stem cells. *Trends Genet.* **13,** 33–39 (1997).
5. Knoblich, J. A. Mechanisms of asymmetric cell division during animal development. *Curr. Opin. Cell Biol.* **9,** 833–841 (1997).
6. Muller, H. A. & Wieschaus, E. *armadillo*, *bazooka* and *stardust* are critical for early stages in formation of the zonula adherens and maintenance of the polarized blastoderm epithelium in *Drosophila*. *J. Cell Biol.* **134,** 149–163 (1996).
7. Kemphues, K. J., Priess, J. R., Morton, D. G. & Cheng, N. S. Identification of genes required for cytoplasmic localization in early *C. elegans* embryos. *Cell* **52,** 311–320 (1988).
8. Etemad-Moghadam, B., Guo, S., & Kemphues, K. J. Asymmetrically distributed PAR-3 protein contributes to cell polarity and spindle alignment in early *C. elegans* embryos. *Cell* **83,** 743–752 (1995).
9. Hung, T. J. & Kemphues, K. J. PAR-6 is a conserved PDZ domain-containing protein that co-localizes with PAR-3 in *Caenorhabditis elegans* embryos. *Development* **126,** 127–135 (1999).
10. Tabuse, Y. *et al.* Atypical protein kinase C cooperates with PAR-3 to establish embryonic polarity in

Caenorhabditis elegans. *Development* **125,** 3607–3614 (1998).
11. Guo, S. & Kemphues, K. J. *par-1*, a gene required for establishing polarity in *C. elegans* embryos encodes a putative Ser/Thr kinase that is asymmetrically distributed. *Cell* **81,** 611–620 (1995).
12. Boyd, L., Guo, S., Levitan, D., Stinchcomb, D. T. & Kemphues, K. J. PAR-2 is asymmetrically distributed and promotes association of P granules and PAR-1 with the cortex in *C. elegans* embryos. *Development* **122,** 3075–3084 (1996).
13. Cheng, N. N., Kirby, C. M. & Kemphues, K. J. Control of cleavage spindle orientation in *Caenorhabditis elegans*: the role of the genes *par-2* and *par-3*. *Genetics* **139,** 549–559 (1995).
14. Watts, J. L. *et al. par-6*, a gene involved in the establishment of asymmetry in early *C. elegans* embryos, mediates the asymmetric localization of PAR-3. *Development* **122,** 3133–3140 (1996).
15. Hartenstein, V. & Campos-Ortega, J. A. Early neurogenesis in wild-type *Drosophila melanogaster*. *Roux's Arch. Dev. Biol.* **193,** 308–325 (1984).
16. Doe, C. Q. Molecular markers for identified neuroblasts and ganglion mother cells in the *Drosophila* central nervous system. *Development* **116,** 855–863 (1992).
17. Bossing, T., Udolph, G., Doe, C. Q. & Technau, G. M. The embryonic central nervous system lineages of *Drosophila melanogaster*: I. Neuroblast lineages derived from the ventral half of the neuroectoderm. *Dev. Biol.* **179,** 41–64 (1996).
18. Kraut, R. & Campos-Ortega, J. A. *inscuteable*, a neural precursor gene of *Drosophila*, encodes a candidate for a cytoskeletal adaptor protein. *Dev. Biol.* **174,** 65–81 (1996).
19. Kraut, R., Chia, W., Jan, L. Y., Jan, Y. N. & Knoblich, J. A. Role of *inscuteable* in orienting asymmetric cell divisions in *Drosophila*. *Nature* **383,** 50–55 (1996).
20. Kuchinke, U., Grawe, F. & Knust, E. Control of spindle orientation in *Drosophila* by the Par-3-related PDZ-domain protein Bazooka. *Curr. Biol.* **8,** 1357–1365 (1998).
21. Wodarz, A., Ramrath, A., Kuchinke, U. & Knust, E. Bazooka provides an apical cue for Inscuteable localization in *Drosophila* neuroblasts. *Nature* **402,** 544–547 (1999).
22. Schober, M., Schaefer, M. & Knoblich, J. A. Bazooka recruits Inscuteable to orient asymmetric cell divisions in *Drosophila* neuroblasts. *Nature* **402,** 548–551 (1999).
23. Yu, F., Morin, X., Cai, Y., Yang, X. & Chia, W. Analysis of *partner of inscuteable*, a novel player of *Drosophila* asymmetric divisions, reveals two distinct steps in Inscuteable apical localization. *Cell* **100,** 399–409 (2000).
24. Lin, D., Gish, G. D., Songyang, Z. & Pawson, T. The carboxyl terminus of B class ephrins constitutes a PDZ domain binding motif. *J. Biol. Chem.* **274,** 3726–3733 (1999).
25. Izumi, Y. *et al.* An atypical PKC directly associates and colocalizes at the epithelial tight junction with ASIP, a mammalian homologue of *Caenorhabditis elegans* polarity protein PAR-3. *J. Cell Biol.* **143,** 95–106 (1998).
26. Sudhof, T. C., Lottspeich, F., Greengard, P., Mehl, E. & Jahn, R. A synaptic vesicle protein with a novel cytoplasmic domain and four transmembrane regions. *Science* **238,** 1142–4 (1987).
27. Johnston, P. A., Jahn, R. & Sudhof, T. C. Transmembrane topography and evolutionary conservation of synaptophysin. *J. Biol. Chem.* **264,** 1268–73 (1989).
28. Garcia, E. P., McPherson, P. S., Chilcote, T. J., Takei, K. & DeCamilli, P. rbSec1 A and B colocalize with syntaxin one and SNAP-25 throughout the axon, but are not in a stable complex with syntaxin. *J. Cell Biol.* **129,** 105–120 (1995).
29. Burbelo, P. D., Drechsel, D. & Hall, A. A conserved binding motif defines numerous candidate target proteins for both Cdc42 and Rac GTPases. *J. Biol. Chem.* **270,** 29071–29074 (1995).
30. Hillier, B. J., Christopherson, K. S., Prehoda, K. E., Bredt, D. S. & Lim, W. A. Unexpected modes of PDZ domain scaffolding revealed by structure of nNOS–Syntrophin complex. *Science* **284,** 812–815 (1999).
31. Colman, D. R. Neuronal polarity and the epithelial metaphor. *Neuron* **23,** 649–651 (1999).
32. Bredt, D. S. Sorting out genes that regulate epithelial and neuronal polarity. *Cell* **94,** 691–694 (1998).
33. Dotti, C. G. & Simons, K. Polarized sorting of viral glycoproteins to the axon and dendrites of hippocampal neurons in culture. *Cell* **62,** 63–72 (1990).
34. Huttner, W. B. & Brand, M. Asymmetric division and polarity of neuroepithelial cells. *Curr. Opin. Neurobiol.* **7,** 29–39 (1997).
35. Van Aelst, L. & D'Souza-Schorey, C. Rho GTPases and signalling networks. *Genes Dev.* **11,** 2295–2322 (1997).
36. Mackay, D. J. G. & Hall, A. Rho GTPases. *J. Biol. Chem.* **273,** 20685–20688 (1998).
37. Hird, S. N. & White, J. G. Cortical and cytoplasmic flow polarity in early embryonic cells of *Caenorhabditis elegans*. *J. Cell Biol.* **121,** 1343–1355 (1993).
38. Hill, D. P. & Strome, S. An analysis of the role of microfilaments in the establishment and maintenance of asymmetry in *Caenorhabditis elegans* zygotes. *Dev. Biol.* **125,** 75–84 (1988).
39. Jou, T. S., Schneeberger, E. E. & Nelson, W. J. Structural and functional regulation of tight junctions by RhoA and Rac1 small GTPases. *J. Cell Biol.* **142,** 101–115 (1998).
40. Kroschewski, R., Hall, A. & Mellman, I. Cdc42 controls secretory and endocytic transport to the basolateral plasma membrane of MDCK cells. *Nature Cell Biol.* **1,** 8–13 (1999).
41. Nakanishi, H., Brewer, K. A. & Exton, J. H. Activation of the ζ isozyme of protein kinase C by phosphatidylinositol 3, 4, 5-trisphosphate. *J. Biol. Chem.* **268,** 13–16 (1993).
42. Standaert, M. L. *et al.* Protein kinase C as a downstream effector of phosphatidylinositol 3-kinase during insulin stimulation in rat adipocytes. Potential role in glucose transport. *J. Biol. Chem.* **272,** 30075–30082 (1997).
43. Self, A. J. & Hall, A. Purification of recombinant Rho/Rac/G25K from *Escherichia coli*. *Methods Enzymol.* **256,** 3–10 (1995).
44. Hart, M. J. *et al.* Cellular transformation and guanine nucleotide exchange activity are catalyzed by a common domain on the *dbl* oncogene product. *J. Biol. Chem.* **269,** 62–65 (1994).
45. Huttner, W. B., Schiebler, W., Greengard, P. & De Camilli, P. Synapsin I (protein I), a nerve terminal-specific phosphoprotein. III. Its association with synaptic vesicles studied in a highly purified synaptic vesicle preparation. *J. Cell Biol.* **96,** 1374–1388 (1983).
46. Hell, J. W. & Jahn, R. in *Cell Biology: a Laboratory Manual* (ed. Celis, J. E.) 567–574 (Academic, San Diego, 1997).
47. Henkemeyer, M. *et al.* Nuk controls pathfinding of commissural axons in the mammalian central nervous system. *Cell* **86,** 35–46 (1996).

ACKNOWLEDGEMENTS

We thank M. Moran and E. Manser for Cdc42 and Rac1 reagents, and R. Steven and T. Kubiseski for technical advice and critical reading of the manuscript. We are indebted to I. Macara and G. S. Martin for sharing unpublished results. D.L. was supported by a graduate studentship from the Medical Research Council (MRC) of Canada. J.F. is an MRC Postdoctoral Fellow. J.D.S. acknowledges support by NIH grant DK44239. This work was supported by the MRC of Canada and by a Howard Hughes Medical Institute Research Scholar Award to T.P. T.P. is a Distinguished Scientist of the MRC of Canada. Correspondence and requests for materials should be addressed to T.P.